https://doi.org/10.5194/gmd-2020-378
Preprint. Discussion started: 26 May 2021

Geoscientific Model Development
Discussions
Open Access
EGU

Turbidity maximum zone index: A novel model for remote extraction of turbidity maximum zone in different estuaries

Chongyang Wang[1‡], Li Wang[1‡], Danni Wang[2], Dan Li[1,3], Chenghu Zhou[1,3,4], Hao Jiang[1,3], Qiong Zheng[1], Shuisen Chen[1], Yangxiaoyue Liu[1,3], Ji Yang[1,3], Xia Zhou[1], and Yong Li[1,3]

[1] Guangdong Open Laboratory of Geospatial Information Technology and Application, Key Lab of Guangdong for Utilization of Remote Sensing and Geographical Information System, Guangzhou Institute of Geography, Guangdong Academy of Sciences, Guangzhou 510070, China

[2] Department of Resources and the Urban Planning, Xin Hua College of Sun Yat-Sen University, Guangzhou 510520, China

[3] Southern Marine Science and Engineering Guangdong Laboratory (Guangzhou), Guangzhou 511458, China

[4] State Key Laboratory of Resources and Environmental Information System, Institute of Geographic Sciences and Natural Resources Research, Chinese Academy of Sciences, Beijing 100101, China

‡ Equally contributed to this work

Correspondence to: Dan Li (lidan@gdas.ac.cn); Chenghu Zhou (zhouch@lreis.ac.cn)

Abstract. Recognizing and extracting estuarine turbidity maximum zone (TMZ) efficiently is important for kinds of terrestrial hydrological process. Although many relevant studies of TMZ have been carried out around the world, the method of extracting and criteria of describing TMZ vary greatly from different regions and

https://doi.org/10.5194/gmd-2020-378
Preprint. Discussion started: 26 May 2021

different times. In order to improve the applicability of the fixed threshold in previous studies and develop a novel model extracting TMZ accurately in multi estuaries and different seasons by remote sensing imagery, this study estimated the total suspended solids (TSS) concentrations and chlorophyll a (Chla) concentrations in Pearl River Estuary (PRE), Hanjiang River Estuary (HRE) and Moyangjiang River Estuary (MRE) of Guangdong province, China. The spatial distribution characteristics of both TSS concentrations and Chla concentrations were analyzed subsequently. It was found that there was an almost opposite relationship between TSS concentration and Chla concentration in the three estuaries, especially in PRE. The regions of high (low) TSS concentrations are exactly corresponding to the relative low (high) Chla concentrations. Based on the special feature, an index named turbidity maximum zone index (TMZI), defining as the ratio of the difference and sum of logarithmic transformation of TSS concentrations and Chla concentrations, was firstly proposed. By calculating the values of TMZI in PRE on 20 November 2004 (low-flow season), it was found that the criterion (TMZI > 0.2) could be used to distinguish TMZs of PRE effectively. Compared with the true (false) color imagery and the rudimentary visual interpretation results, the TMZs extraction results by TMZI were mostly consistent with the actual distribution. Moreover, the same criterion was further applied in PRE on 18 October 2015. The high accuracy and good consistency across seasons were also found. The west shoal of PRE was the main distribution areas of TMZs. In addition, the good performance in extracting TMZs by this newly proposed index were also found in different estuaries and different times (HRE, 13 August 2008, high-flow season; MRE, on 6 December 2013, low-flow season). Compared to the previous fixed threshold (TSS or turbidity) methods, extracting TMZ by TMZI has a higher accuracy and better applicability. Evidently, this unified TMZI is a potentially optimized method to monitor and extract TMZs of other estuaries in the world by different satellite remote sensing imageries, which can be used to improve the understanding of the spatial and temporal variation of TMZs and estuarial processes on regional and global scales, and the management and sustainable development of regional society and nature environment.

Keywords: turbidity maximum zone; turbidity maximum zone index; total suspended solid; chlorophyll a; remote sensing; estuary

1 Introduction

Turbidity maximum zone (TMZ) is the dynamic turbid water areas within limits in estuary, where the suspended solids (sediment, matter) concentrations are steadily and significantly higher than landward and seaward (Shen, 1995; Gebhardt et al., 2005; Yu et al., 2014; Li et al., 2019; Wang et al., 2020a). It is a special phenomenon of the progress of suspended sediment movement and migration in estuary throughout the world (Schubel, 1968; Shi et al., 1993; Mitchell et al., 2012; Wang et al., 2020b). The spatial distributions and dynamic change of TMZs not only have a deep and wide impact on the formation and development of estuary morphology, channel, shoal and sandbar (Asp et al., 2018; Azhikodan and Yokoyama, 2019; Li et al., 2019), but also

https://doi.org/10.5194/gmd-2020-378
Preprint. Discussion started: 26 May 2021

affect the physics, geochemical and biogeochemical processes of estuarine nature environment as well as social production activities significantly(Gebhardt et al., 2005; Jalón-Rojas et al., 2016; Kitheka et al., 2016; Toublanc et al., 2016; Yan et al., 2020). It could be found that TMZ has long been a hot topic for scientific inquiries and engineering innovations among a broad spectrum of scholars, government agencies, engineering corporations, and communities (Shen et al., 2001; Shi et al., 2017; Jiang et al., 2019; Wang et al. 2020a).

Previous works have studied TMZ from various aspects based on different data resources and methods, such as the characteristics and dynamics of total suspended solids (TSS) concentrations in TMZs (Yang et al., 2014; Wan and Wang, 2017; Grasso et al., 2018), the mechanisms and formation of TMZ (Brenon and Hir, 1999; Wai et al., 2004; Yu et al., 2014; Toublanc et al., 2016), the location, distribution and change of TMZs across the time (Jiang et al., 2013;Jalón-Rojas et al., 2016; Li et al., 2019; Yan et al., 2020), the interaction with other factors and its long-term trend (Gebhardt et al., 2005; Chen et al., 2016; Li et al., 2019). It should be noted that where a TMZ is located in an estuary is a fundamental question and an important task for studying TMZ. It was found that there were two major ways to obtain the locations and distributions of TMZs in current studies (Wang et al., 2020a). One was relatively rough description, such as the locations of TMZ correspond to the front of salinity wedge and moving range of stagnation points, or a distance from coastlines (Feng et al., 2002; Mitchell, 2013; Kitheka et al., 2016; Liu et al., 2016; Toublanc et al., 2016; Gong et al., 2017; Zhang et

https://doi.org/10.5194/gmd-2020-378
Preprint. Discussion started: 26 May 2021

al., 2019; Yan et al., 2020). Another was relatively quantitative result, extraction of TMZs was conducted by some types of thresholds of TSS concentrations or turbidity criterion (Jiang et al., 2013; Yang and Liu, 2015; Chen et al., 2016; Jalón-Rojas et al., 2016; Shi et al., 2017; Li et al., 2019). However, the above mentioned fixed threshold method has its latent deficiencies. It is a challenging job to generate precisely TMZs extraction results in different time by a fixed threshold of TSS concentration because TSS concentrations showed remarkable variations in different seasons. Moreover, the threshold values are difficult to be transplanted from local regions to other regions and researches due to lacking of scientific basis. The threshold method and criteria varied greatly in different estuaries, in different regions of a same estuary, in same estuary at different time and by different studies, which showed considerable subjectivity. The results are not comparable (Wang et al., 2020a).

TSS concentrations in TMZs and adjacent waters have a significant variation (Uncles et al., 2000; Park et al., 2008; Mitchell, 2013; Wang et al., 2018). And many studies have proved that suspended solids could affect the growth of chlorophyll a (Chla) through absorbing and scattering of the sunlight in water areas (Pozdnyakov et al., 2005; Chen et al., 2015; Montanher et al., 2014; Wang et al., 2017a; Wang et al., 2020b). Therefore, we conclude that there is a relationship between TSS concentrations and Chla concentrations and different characteristics in TMZs and normal water bodies in estuary, which might be used to overcome the drawbacks of previous methods of extracting TMZ, and distinguish and recognize TMZ effectively.

https://doi.org/10.5194/gmd-2020-378
Preprint. Discussion started: 26 May 2021

Based on the above analysis, the objectives of this study are to propose a new model with better adaptability and robustness for distinguishing and extracting TMZ in different estuaries and different seasons. To achieve this goal, the TSS concentrations and Chla concentrations in three estuaries (Pearl River Estuary, PRE; Hanjiang River Estuary, HRE; Moyangjiang River Estuary, MRE) were estimated firstly. And the different spatial characteristic of them were further analyzed and compared. Subsequently, the corresponding relationship and special feature between TSS concentration and Chla concentration were fully used to develop a turbidity maximum zone index (TMZI). Finally, this study extracted TMZs in these estuaries at different time by the model (TMZI), and validated and assessed its accuracy.

The paper is arranged as follows. The study areas, in situ data, satellite imagery, TSS concentration data were described along with Chla retrieval model and its calibration and validation in Section 2. The spatial analysis of TSS concentration, Chla concentration and the corresponding relationship between them were presented in Section 3.1. The establishment of TMZI and its application and assessment in different estuaries and different times were showed in Sections 3.2-3.5. Finally, the summary and conclusions were given in Section 4.

https://doi.org/10.5194/gmd-2020-378
Preprint. Discussion started: 26 May 2021

Geoscientific Model Development
Discussions
Open Access

2 Dataset and methods

2.1 Study areas

The study areas include Pearl River Estuary, Hanjiang River Estuary and Moyangjiang River Estuary of Guangdong province, South China (Fig. 1, Fig. 4 and Figs. 7-10). The PRE is located between longitudes 113.45°-114.2°E and latitudes 22.25°-22.85°N mainly in the core zone of Guangdong-Hong Kong-Marco Greater Bay Area, Southern Guangdong province; HRE is located between longitudes 116.6°-117°E and latitudes 23.2°-23.6°N mainly in Shantou city, Eastern Guangdong province; while MRE is located between longitudes 111.9°-112.3°E and latitudes 21.66°-21.8°N mainly in Yangjiang city, Western Guangdong province. Among them, Pearl River has the second large annual runoff and is the third largest river in China. Hanjiang River and Moyangjiang River are the second and third large and famous rivers in Guangdong province (Chen et al., 2011; Wang et al., 2017a; Wang et al., 2018; Wang et al., 2020b). Previous studies reported that the sediment load of them are $7.53 \cdot 10^7$, $6.93 \cdot 10^6$ and $3.27 \cdot 10^5$ ton per year on average (Wang et al., 2017a, b; Wang et al., 2020). It could be found that TMZs often develops in these estuaries and many associated research work has been carried out in the regions for a long time, especially in PRE.

https://doi.org/10.5194/gmd-2020-378
Preprint. Discussion started: 26 May 2021

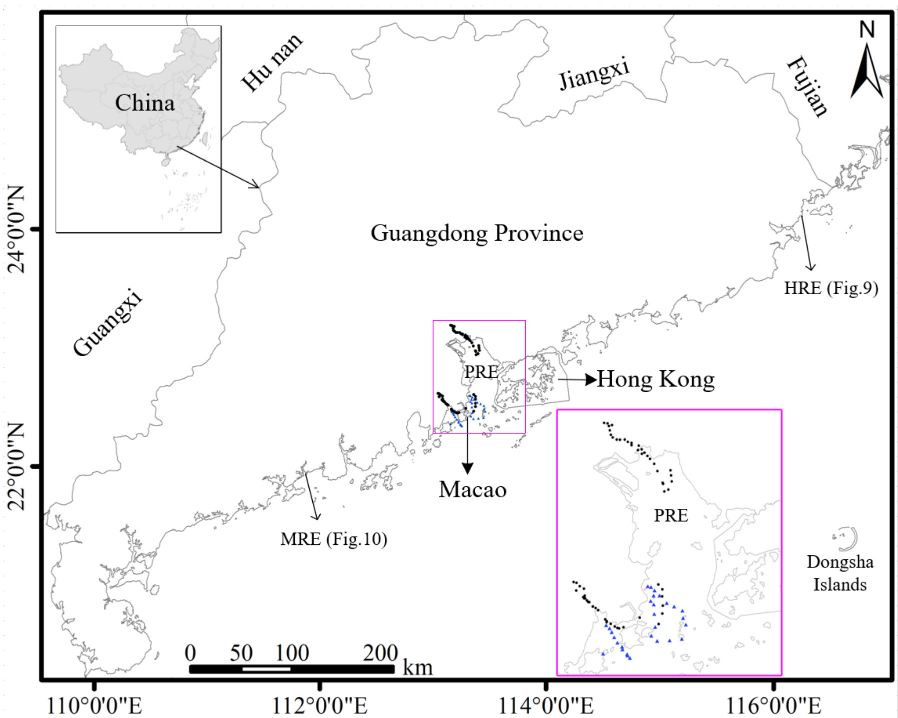

Fig. 1. Study areas (PRE, HRE, MRE) and the locations of in situ data (black dots and blue triangles).

2.2 In-situ and satellite data

The 89 in-situ samples including the reflectance of water surface and Chla concentrations were all collected from PRE, shown in Fig. 1 (black dots and blue triangles). Among them, 60 samples (Fig. 1, black dots; Table 1) were same as our previous work (Chen et al., 2011). This study added newly other 29 samples (Fig. 1, blue triangles; Table 1). The above-mentioned samples were used to recalibrate and validate a Landsat-based Chla concentration retrieval model in this study.

Besides, four scenes of Landsat imageries with good quality were used in the study. Two scenes of image from TM and OLI (path/row = 122/44) was captured on 20

https://doi.org/10.5194/gmd-2020-378
Preprint. Discussion started: 26 May 2021

Geoscientific Model Development
Discussions

November 2004 and 18 October 2015, respectively, covering PRE (Fig. 7a and Fig. 8c). The other one of them from OLI (path/row = 120/44) was captured on 13 August 2008, covering HRE (Fig. 9c). The last one from OLI (path/row = 123/45) as well, was captured on 6 December 2013, covering MRE (Fig. 10c).

Table 1

Information about the 89 in-situ data.

Date	Samples	Measurements	
Dec 9, 2006	16	Reflectance, Chla	
Dec 21, 2006	12	Reflectance, Chla	Same as
Dec 27, 2007	15	Reflectance, Chla	Chen et al. (2011)
Dec 31, 2007	17	Reflectance, Chla	
Nov 2, 2012	18	Reflectance, Chla	Newly added
Sep 10, 2013	11	Reflectance, Chla	

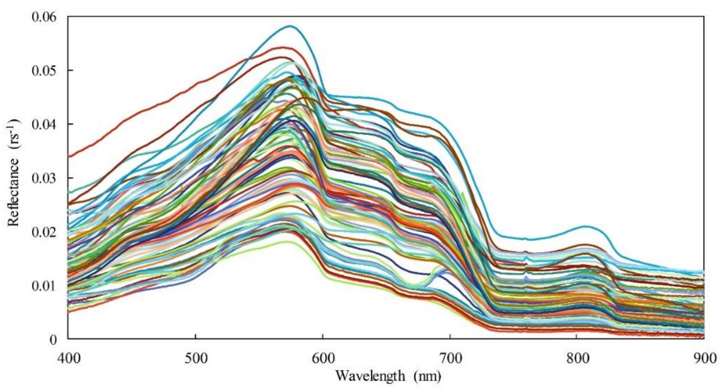

Fig. 2. Remote sensing reflectance of surface water of the 89 in situ data.

2.3 Total suspended solids data and chlorophyll a data

This study intends to establish and develop a new model (TMZI) based on TSS concentrations and Chla concentrations, and further extract TMZs in three estuaries of Guangdong province. Therefore, the results of TSS concentrations and Chla concentrations in the study areas should be calculated firstly. For the TSS concentrations data, the results were obtained from our previous works directly (Wang et al., 2017a, b; Wang et al., 2018; Wang et al., 2020). However, the corresponding Chla data needs to be retrieved by Landsat imagery. Consequently, a Landsat-based Chla concentration retrieval model applicable to estuaries of Guangdong province is expected. It can be found that many models have been developed for estimating Chla concentration from different remote sensing data (Gregg and Casey, 2004; Chen et al., 2011; Kim et al., 2016a, b; Attila et al., 2018). Following the feature and form of some typical chlorophyll a retrieval models (Le et al., 2009; Chen et al., 2011; Le et al., 2013; Song et al., 2013), this study recalibrated and validated a three band Landsat-based chlorophyll a model using the 89 in-situ samples (Fig. 3; Equation 1). The model based on Landsat TM and OLI sensors explained about 80% of the Chla concentration variation (Chla: 1.92-92.6 mg/m^3, N=60, P-value<0.01) and had an acceptable validation accuracy (Chla: 2.33-36.8 mg/m^3, RMSE$\leqslant$3.76 mg/m^3, N=29).

https://doi.org/10.5194/gmd-2020-378
Preprint. Discussion started: 26 May 2021

Geoscientific Model Development Discussions

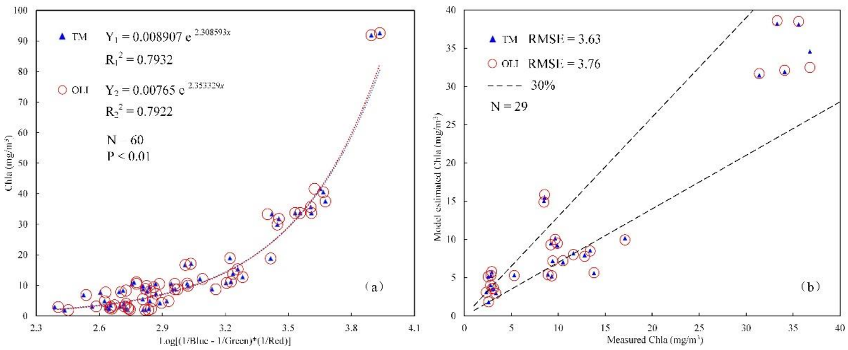

Fig. 3. The calibration (a) and validation (b) results of Chla retrieval models based on 89 in situ data for Landsat sensors.

$$Chla = a * e^{b*Log[(\frac{1}{R_1}-\frac{1}{R_2})*\frac{1}{R_3}]} \qquad (1)$$

Where, R_1, R_2 and R_3 represent blue, green, and red band of TM and OLI sensors. Parameters a and b corresponding to TM and OLI sensors are 0.008907, 2.308593 and 0.00765, 2.353329, respectively. The unit of chlorophyll a concentration is in mg/m^3.

3 Results and discussion

3.1 The spatial characteristic of TSS concentrations and Chla concentrations in estuaries

This study estimated the results of Chla concentrations in each estuary through the developed Chla concentrations retrieval model (Fig. 3). The different spatial distribution characteristics of TSS concentrations and Chla concentrations were analyzed, respectively. Take PRE as an example, it was found that TSS concentrations in low-flow season of PRE (20 November 2004) with a large variation ranging from 1.37 mg/L to more than 200 mg/L (Fig. 4a). Due to the strong interaction between runoff

https://doi.org/10.5194/gmd-2020-378
Preprint. Discussion started: 26 May 2021

and tide, the main region of high TSS concentrations concentrates on west shoal of PRE (Wang et al., 2018), where the TSS concentrations more than 100 mg/L were frequently found. Besides, TSS concentrations in part of east shoal and Neilingding island adjacent waters were also with relative higher value. The other areas of PRE has low TSS concentrations, where the maximum value is general not more than 40 mg/L, especially in Hongkong coastal water bodies (Fig. 4a).

Different from TSS concentrations results, the Chla concentrations in PRE are with much lower value (less than 20 mg/m^3 in almost whole PRE) (Fig. 4b). The results was consistent with the findings of Liu et al. (2017) and Huang et al. (2005), which showed Chla concentrations ranged from 0.24 mg/m^3 to 21.5 mg/m^3 in PRE at different time. In addition, it was found that Chla concentrations in PRE showed an almost opposite spatial characteristics compared to TSS concentrations. Except for eastern Lidao district coastal water bodies, the regions of relative high (low) Chla concentrations are exactly the regions of relative low (high) TSS concentrations. These corresponding features are obvious in the four water ways (Humen, Jiaomen, Hongqimen, Hengmen), shoals and channels of PRE (Fig. 4).

https://doi.org/10.5194/gmd-2020-378
Preprint. Discussion started: 26 May 2021

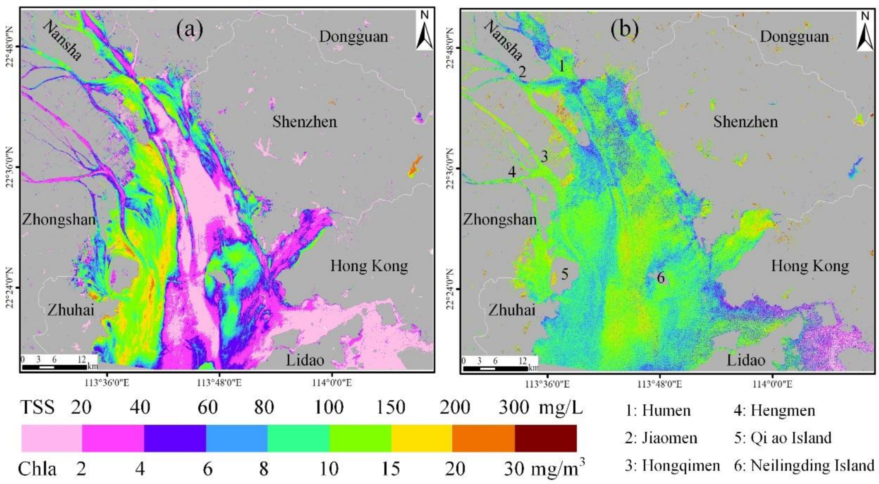

Fig. 4. Estimated TSS concentrations (a) and Chla concentrations (b) in HRE on 20 November 2004.

For further analyzing and assessing the corresponding relationship between TSS concentrations and Chla concentrations in estuary, this study extracted three rows (Fig. 7a; pink lines; rows 1200, 1600, and 1900, columns from 800 to 1300) of TSS concentrations and Chla concentrations values in PRE. The results of row 1600 was shown in Fig. 5(a). The correlation analysis showed remarkable negative correlation of TSS concentrations and Chla concentrations. For the original TSS concentrations and Chla concentrations, the correlation coefficient is -0.6531. While the correlation coefficient reaches about -0.9 for its trend lines (Fig. 5a).

3.2 Establishment and application of TMZI

Based on the above analysis and the corresponding features between TSS concentrations and Chla concentrations, we consider that a transform results deriving from the two water color elements may help distinguishing and extracting TMZ better.

Then, this study defined a TMZI as the ratio of the difference and sum of logarithmic transformation of TSS concentrations and Chla concentrations (equation 2) referring to the other remote sensing indexes, such as Normalized Difference Vegetation Index.

$$TMZI = [Log(TSS) - Log(Chla)] \ / \ [Log(TSS) + Log(Chla)] \qquad (2)$$

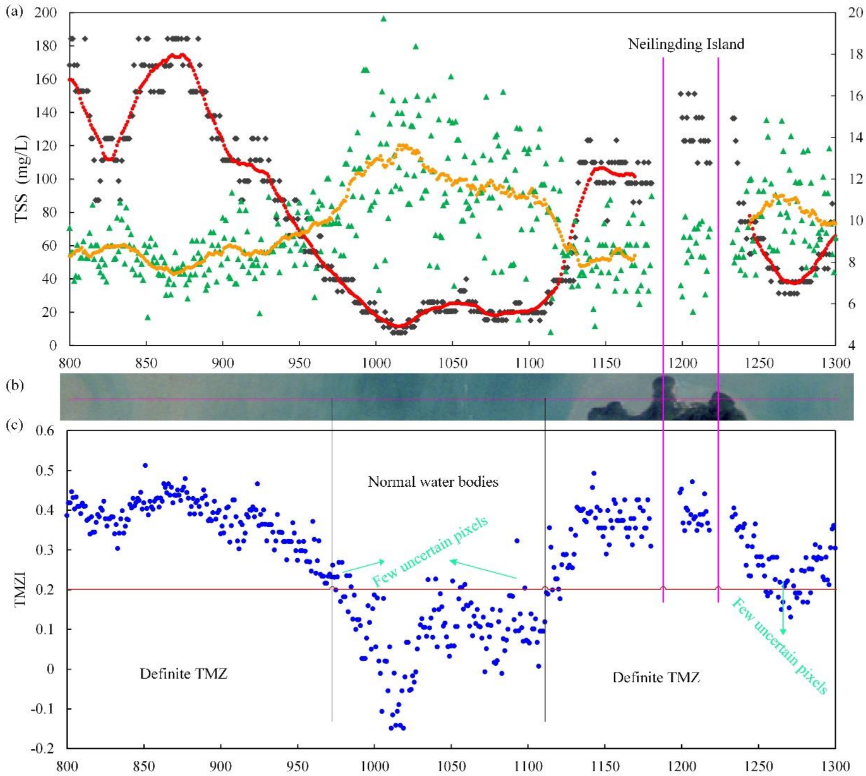

Fig. 5. The spatial corresponding relationship between the TSS concentrations (black dots, red trend line) and Chla concentrations (green triangles, orange trend line) of row 1600 (a), the true color imagery (b) and the corresponding values of TMZI (c).

According to the definition and equation, this study calculated the above mentioned corresponding rows TMZI values (Fig. 5c, Fig. 6b and Fig. 6d). Take the results of row 1600 as an example (Fig. 5b and Fig. 5c), the row pixels could be mainly

https://doi.org/10.5194/gmd-2020-378
Preprint. Discussion started: 26 May 2021

divided into one TMZ (columns from 800 to 975), normal water bodies (columns from 975 to 1110) and another TMZ (columns from 1110 to 1300) from left to right. The null data located at columns 1180-1200 and 1220-1235 are Neilingding Island (Fig. 5, Fig. 7a). Through the comparison to the results of TMZI, it was found that all the values of TMZI corresponding to TMZ pixels are bigger than 0.2 while the values corresponding to normal water bodies pixels are all smaller than 0.2, except for very few blurry pixels (Fig. 5b and Fig. 5c). For the results of rows 1200 and 1900, the similar corresponding characteristics between TMZ and TMZI, and the same criterion were also found (Fig. 6). Hence we can read that TMZI showed a significant feature and had potential to develop into a better model for recognizing and extracting estuarine TMZ more effectively.

https://doi.org/10.5194/gmd-2020-378
Preprint. Discussion started: 26 May 2021

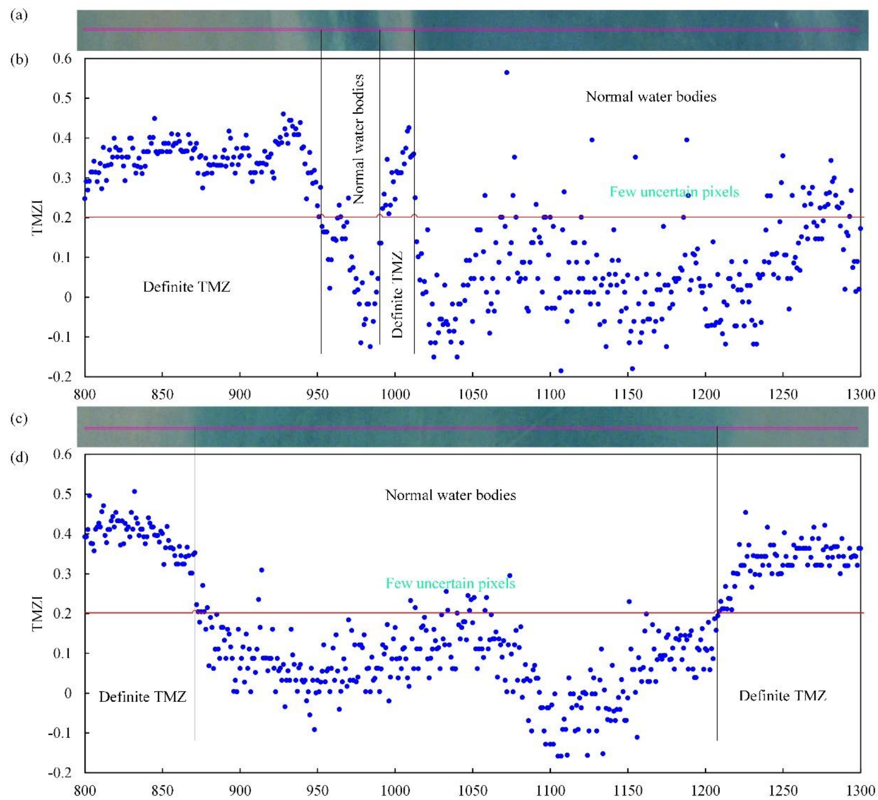

Fig. 6. The true color imagery and the corresponding values of TMZI of rows 1200 (a, b) and 1900 (c, d).

After that, TMZI of the whole Landsat TM imagery was calculated and TMZs in PRE were extracted. Fig. 7(b) showed the spatial distribution results of TMZ in PRE on 20 November 2004 (regions with mango colors). It was found that TMZ is widely distributed throughout PRE, accounting for more than half of water areas in the imagery. Among them, a main TMZ was located within an average distance of 11 km from Panyu, Nansha, Zhongshang and Zhuhai coasts, which is roughly corresponding to the west shoal in PRE. In western Dongguan and Shenzhen coastal water bodies, an approximately rectangular TMZ was developed (within a distance of about 5 km from coastline), where the East Shoal frequently appears in PRE (Wang et al., 2018). Besides, a third main TMZ in PRE located from surrounding Neilingding Island to western Hong Kong water bodies was been found, although TSS concentrations in the TMZ were lower than that of the former TMZs (Fig.4 a and Fig.7 b). Compared to the preliminary diagrams in our previous works (Fig.7 a) (Wang et al., 2020a, b), it was found that the extracted TMZ results by TMZI in this study got a better accuracy and more natural, which indicates a more effective way to recognize TMZs in estuaries (Figs. 6-7).

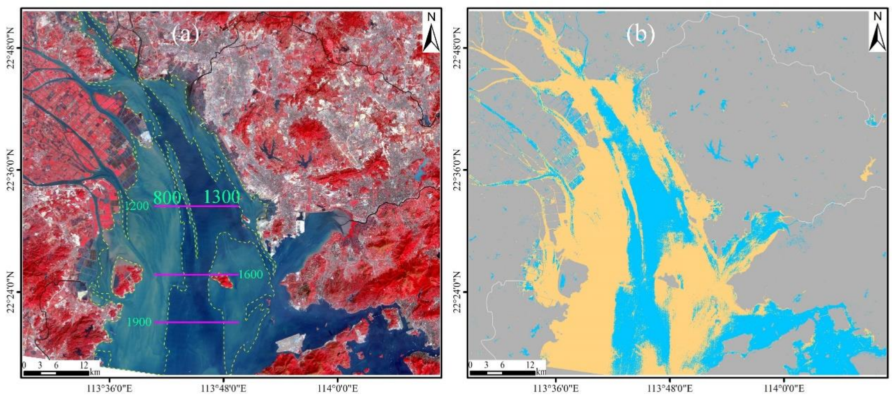

Fig. 7. False color imagery (USGS 1982; NASA 2001), rough spatial distributions (yellow dashed frames) of TMZ (Wang et al., 2020a, b) (a), and the extracted TMZ results (regions with mango colors) by TMZI (b) in PRE on 20 November 2004 (low-flow season)..

3.3 Validation of the accuracy of TMZI in different seasons

Due to the complexity of hydrodynamic environments, estuarine factors and water color elements showed great variations in different seasons, even in the same estuary at

https://doi.org/10.5194/gmd-2020-378
Preprint. Discussion started: 26 May 2021

Geoscientific Model Development
Discussions
Open Access
EGU

the different time of the day. Therefore, this study further validated the accuracy of TMZI of extracting TMZ in PRE in the high-flow season (18 October 2015).

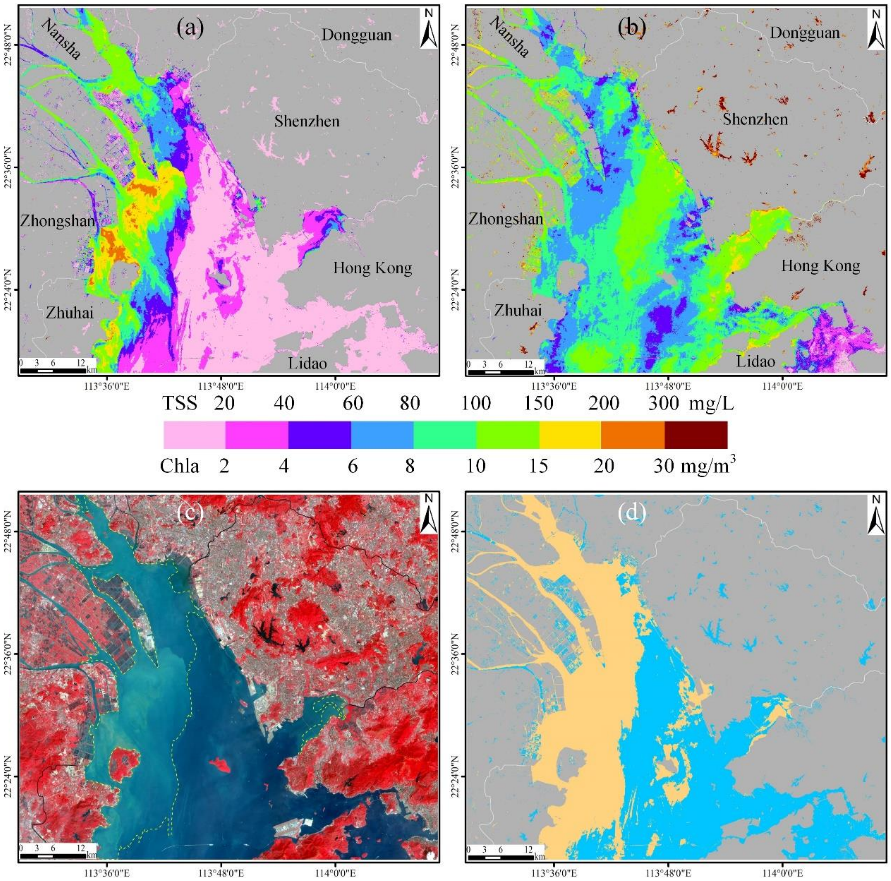

Fig. 8. The estimated TSS concentrations (a), Chla concentrations (b), false color imagery (USGS 1982; NASA 2001), rough spatial distributions (yellow dashed frames) of TMZ (Wang et al., 2020b) (c), and extracting TMZ results (regions with mango colors) by TMZI (d) in PRE on 18 October 2015 (high-flow season).

Fig. 8(a) and Fig. 8(b) showed the retrieved TSS concentrations and Chla concentrations results in high-flow season of PRE. It is clearly that the results in

https://doi.org/10.5194/gmd-2020-378
Preprint. Discussion started: 26 May 2021

different sesaon had big difference (Fig. 4 and Fig. 8). On 18 October 2015, TSS concentrations in PRE had wider variables, ranging from 2.23 to 286.6 mg/L. However, the water bodies with high TSS concentrations (more than 80 mg/L) were mainly in the outlets of four waterways (Humen, Jiaomen, Hongqimen and Hengmen). The other areas of PRE had much lower TSS concentrations, where the TSS concentrations were less than 20 mg/L generally (Fig. 8a). Similar to the corresponding features between TSS concentrations and Chla concentrations in low-flow season, the almost opposite spatial characteristics still existed in high-flow season. For regions with relative high (low) Chla concentrations where showed relative low (high) TSS concentrations (Fig. 8a and b). But it shoud be noted that eastern Lidao district coastal water bodies were an exception, which same to the results in low-flow season (Fig. 4). Both TSS concentrations and Chla concentrations in the zone were relative low (Fig. 4 and Fig. 8).

Based on the resluts of TSS concentrations and Chla concentrations of PRE on 18 October 2015, the study calculated TMZI and extracted TMZs of PRE in high-flow season (Fig. 8d; regions with mango colors). In comparison with the rough diagram results by the original imagery directly (Fig.8 c) (Wang et al., 2020b), the newly extracted TMZs in this study showed a higher accuracy and agreed better with the reality. It was found that there remained only one main TMZ along the west coast of PRE (Fig. 8d), which similar to one of the main TMZs in low-flow season 2004 (Fig. 7b). However, there still exisited obvious difference at different seasons, such as TMZs

https://doi.org/10.5194/gmd-2020-378
Preprint. Discussion started: 26 May 2021

Geoscientific Model Development Discussions

in Hongqimen and Hengmen waterways and eastern Zhuhai coasts (Fig. 7b and Fig. 8d). The other TMZs in high-flow season 2015 were mainly located in the sourronding Dachanwan Wharf of Shenzhen and Neilingding Island. The distributions were obvious less than them in low-flow season 2004 (Fig. 7b). Besides, two relative small isolated TMZs could be found at western two artificial islands of the Hong Kong-Zhuhai-Macao Bridge (Fig. 8d), respectively, which may imply the associated influence of human activities.

According to the analysis of results in PRE on 18 October 2015, it indicated that the TMZI and the criterion (TMZI > 0.2) also worked well in extracting esturaine TMZ in different seasons by Landsat OLI imagery.

3.4 Assessment of the applicability of TMZI in different estuaries

In order to further assess the applicability of TMZI in different estuaries, the corresponding TMZs results in HRE and MRE were also calculated and validated, similar to PRE.

https://doi.org/10.5194/gmd-2020-378
Preprint. Discussion started: 26 May 2021

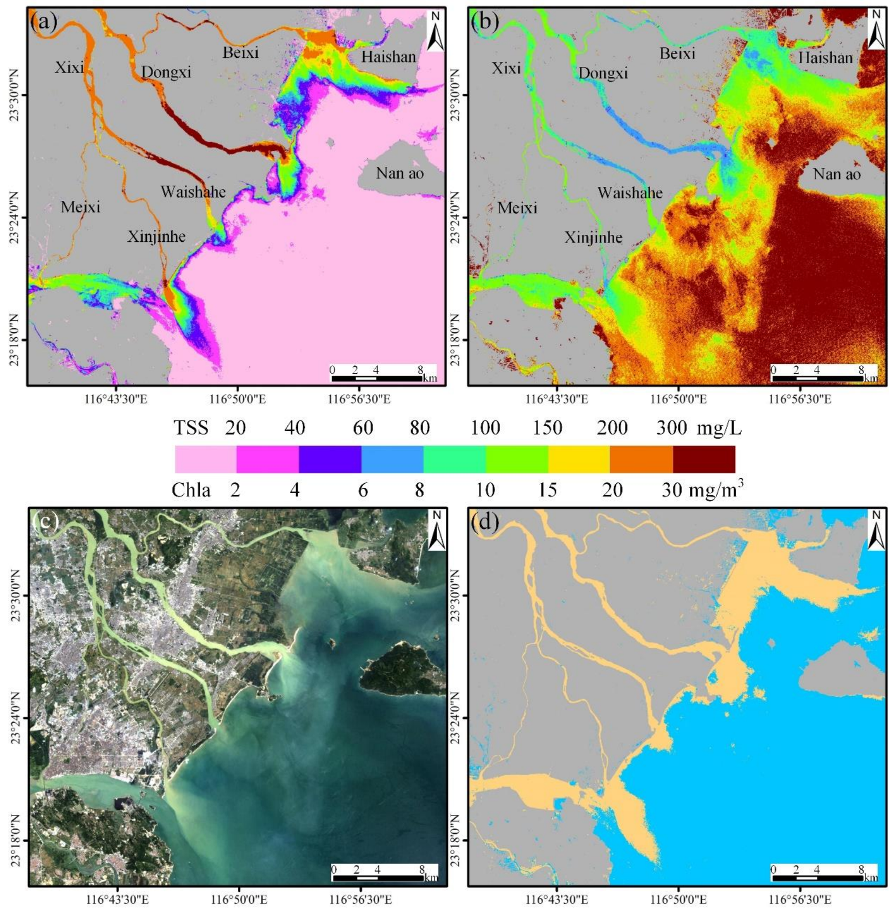

Fig. 9. The estimated TSS concentrations (a), Chla concentrations (b), true color imagery (USGS 1982; NASA 2001) (c), and extracted TMZ results (regions with mango colors) (d) in HRE on 13 August 2008 (high-flow season).

Fig. 9(a) and Fig. 9(b) showed the results of TSS concentrations and Chla concentrations in HRE on 13 August 2008. It is clear that the TSS concentrations in downstream and estuary of HRE are much higher than outer shelf area, especially in the downstream of Dongxi River and Xinjinhe River waterways of Hanjiang River, with a mean value of even more than 300 mg/L (Fig. 9 a). TSS concentrations in the offshore

https://doi.org/10.5194/gmd-2020-378
Preprint. Discussion started: 26 May 2021

area (South China Sea) were less than 20 mg/L frequently. Hence, a significant decreasing trend of TSS concentration could be found from the northwest to southeast in HRE (Fig. 9 a). Besides, the Chla concentrations in HRE showed an opposite spatial distributions characteristics, which similar to the findings in PRE (Fig. 4 and Fig. 8). In general, relative low Chla concentrations were mainly found in downstream and estuary while outer shelf area with high values (Fig. 9 b). Chla concentrations in HRE ranged from 4.1 to 37.3 mg/m^3 (Fig. 9 b), which were a little higher than that of PRE (Fig. 4 and Fig. 8).

The results of extracted TMZs in HRE were showed in Fig. 9(d) (regions with mango colors). We found that the TMZs distributed in all downstream and estuary of Hangjiang River. They could be devided into four main TMZs based on different waterways (Beixi, Dongxi, Waishahe, Xinjinhe and Meixi waterways) of Hanjing River. The maximum TMZ was located within an average distance of 3 km from Beixi estuary, western Haishan coasts and the coastlines between Beixi and Dongxi esturay. From Meixi estuary to Xinjinhe estuary, the second large TMZ of HRE was distributed. The region of the main TMZ of Xinjinhe estuary looks knife-shaped, which was mainly caused by the runoff of Xinjinhe waterway and the flow guiding line connected to Longhu District, Shantou City (Fig. 9 d). The other two relative smaller TMZs were distributed in Dongxi estuary and Waishahe estuary, respectively. The results indicated that the TMZs distribution in HRE mainly connected to tide, runoff, estuarine

https://doi.org/10.5194/gmd-2020-378
Preprint. Discussion started: 26 May 2021

topography and human activity. We found that TMZI has a high applicability in a different eatuary beside PRE.

While in HRE, the region of high TSS concentrations were mainly distributed in an average distance of 1.2 km from Yangjiang coastlines, especially in eastern Hailingdati dike water bodies, with a mean value of more than 150 mg/L (Fig. 10a). The outer shelf area has much lower TSS concentrations, where the TSS concentrations were less than 35 mg/L generally. It was also found that Chla concentrations in most region of MRE were more than 4 mg/m^3, except for southwestern Dongping town coastal water bodies where Chla concentrations main ranged from 2 to 4 mg/m^3. Chla concentrations in Moyangjiang River downstream, Fuchang town coast and outside of Shouchanghe River estuary have relative high values where Chla concentrations more than 8 mg/m^3 were often found (Fig. 10b). Compared to PRE and HRE, the corresponding relationship between TSS concentrations and Chla concentrations in MRE was a little weak. However, there still existed a trend that high (low) TSS concentrations water bodies with relative low (high) Chla concentrations (Fig. 10a and Fig. 10b).

https://doi.org/10.5194/gmd-2020-378
Preprint. Discussion started: 26 May 2021

Geoscientific Model Development
Discussions

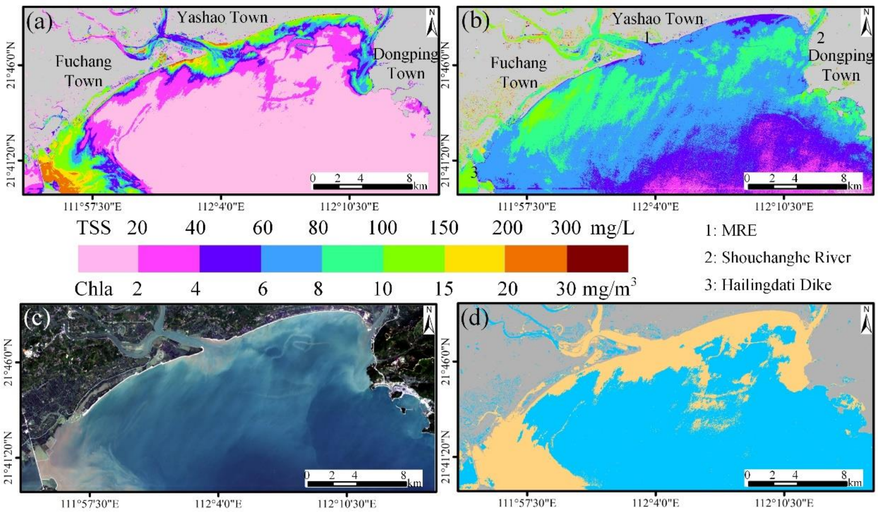

Fig. 10. The estimated TSS concentrations (a), Chla concentrations (b), true color imagery (USGS 1982; NASA 2001) (c), and extracted TMZ results (regions with mango colors) (d) in MRE on 6 December 2013 (Low-flow season).

Fig. 10(c) and Fig. 10(d) showed the ture color imagery of MRE and the extracted TMZs results (regions with mango colors). It was found that there were two main TMZs in MRE on 6 December 2013. The first TMZ mainly distributed from inside and outside of Moyangjiang River estuary to Shouchanghe River estuary, with a distance of about 1.8 km from coastlines (Fig. 10 d). The TMZ distribution in this region mainly attribute to interaction of tide and runoff. Another mian TMZ was in the regions with a distance of 4 km from Hailingdati dike, which mainly caused by the obstruction agains ocean currents of Hailingdati dike (Fig. 10 d). In addition, it was clear that several small long narrow TMZs were also accuracy extreacted through TMZI and the same criterion as that in PRE and HRE. All the results in the three estuaries showed that extracting TMZ

https://doi.org/10.5194/gmd-2020-378
Preprint. Discussion started: 26 May 2021

based on TMZI and the criterion (TMZI > 0.2) has a better applicability in multi eatuaries.

3.5 TMZI compared to fixed threshold criterion of previous studies

As the above mentioned, previous studies extracts TMZ mainly based on threshold of TSS concentrations or turbidity. For example, Jalón-Rojas et al. (2016) used thresholds of 500 mg/L (300 NTU) and 1000 mg/L (600 NTU) to define moderately-concentrated TMZ and highly-concentrated TMZ in France Loire Estuary; Jiang et al. (2013) and Li et al. (2019) defined TMZ as the areas with TSS values larger than 700 mg/L in Yangtze Estuary and Hangzhou Bay. While for the TMZ in PRE, it was found that TSS values in studies of Shi et al. (2017) and Wai et al. (2004) were more than 89.4 mg/L and about 150 mg/L, respectively. Based on the two criteria (TMZ: TSS > 89.4 mg/L or TSS > 150 mg/L), this study calculated and extracted TMZs in PRE. The results were showed in Fig. 11(c-f), regions with cyan or yellow colors.

It was easy to find that the extracted TMZs results in PRE based on the criterion of Shi et al. (2017) were better that of Wai et al. (2004), no matter on 20 November 2004 (Fig. 11c vs. Fig. 11e, low-flow season) or 18 October 2015 (Fig. 11d vs. Fig. 11f, high-flow season). The main reason might be that the time of data source in Shi et al. (2017) was more close to our study than that in the study of Wai et al. (2004), which causes that the criterion of Shi et al. (2017) was more suitable to this study than that of Wai et al. (2004).

https://doi.org/10.5194/gmd-2020-378
Preprint. Discussion started: 26 May 2021

Geoscientific Model Development
Discussions
Open Access

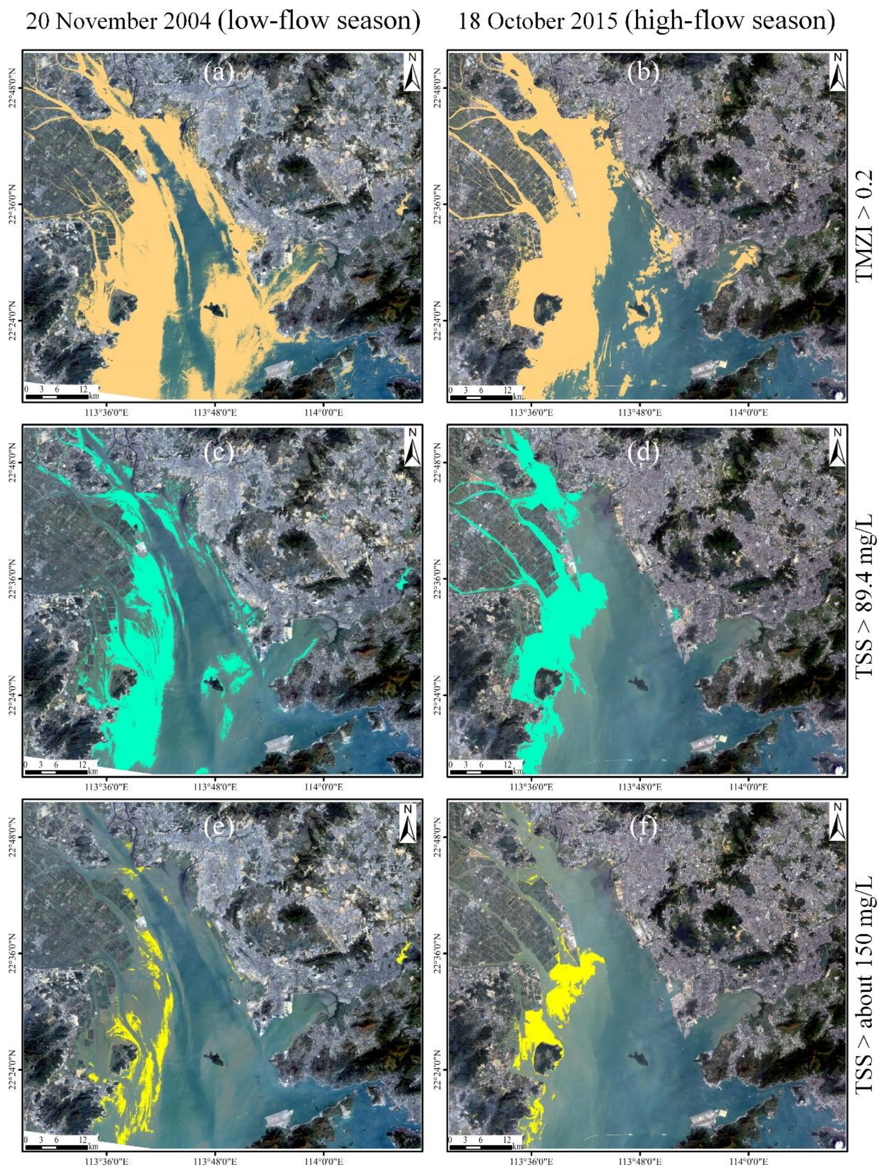

Fig. 11. TMZ results in PRE at different time (a, c, e: 20 November 2004; b, d, f: 18 October 2015; (USGS 1982; NASA 2001)) based on TMZI method by this study (a, b, regions with mango color; same as Fig. 7b and Fig. 8d), the criterion by Shi et al. (2017) (c, d, regions with cyan color), and the criterion by Wai et al. (2004) (e, f, regions with yellow color), respectively.

Besides, it was also found that a relative good result was obtained in the west shoal of PRE on 20 November 2004 by the criterion of Shi et al. (2017) (Fig. 11c). The extracted TMZs were almost consistent with the reality compared to the true color imagery and our rudimentary visual interpretion results (Wang et al., 2020a, b). However, the accuracy in the east shoal and surrounding Neilingding Island of PRE was not as high as that in the west shoal, where much obvious distributions of TMZs were not recognized effectively (Fig. 11c). What is worse, it was found that the same criterion did not work well in the west shoal of PRE at a different time (Fig. 11c vs. Fig. 11d). Almost a third of the distributions of TMZs in the west shoal of PRE on high-flow season was not distinguished and extracted (Fig. 11d). The results based on the criteria of previous studies indicated that fixed thresholds have a distinct disadvantage when extracting TMZ in different times or estuaries.

Based on the evaluation and analysis of all the above results (Figs. 7-11), we can find that the TMZI could be widely and effectively applied to the accurate extraction of estuarine TMZ, regardless of the significant variations of hydrodynamic environments, TSS concentrations, Chla concentrations in different estuaries and seasons. Compared to the previous studies and the results from fixed thresholds, we conclude that TMZI has the great potential to develop into a unified model for distinguishing and extracting TMZ effectively and accurately in many other estuaries of the world (Figs. 7-11).

https://doi.org/10.5194/gmd-2020-378
Preprint. Discussion started: 26 May 2021

4 Summary and Conclusions

This study established and developed a novel model (turbidity maximum zone index) based on TSS concentration and Chla concentration for distinguishing estuarine turbidity maximum zone from Landsat imageries. It was found that both TSS concentration and Chla concentration showed significant variations and different characteristics in PRE, HRE and MRE in different times (Fig. 4 and Figs. 8-10). However, we found that there still exists a corresponding relationship between TSS concentration and Chla concentration in the three estuaries of Guangdong province. Chla concentrations and TSS concentrations in this study showed an almost opposite spatial distributions characteristics, where relative high (low) Chla concentrations are exactly corresponding to the relative low (high) TSS concentrations (Figs. 4-5 and Figs. 8-10). Therefore, the turbidity maximum zone index (TMZI) was defined and designed as the ratio of the difference and sum of logarithmic transformation of TSS concentrations and Chla concentrations in this study.

Compared with the true (false) color imagery or visual interpretation results, it was found that the extracted TMZs results by TMZI were consistent with the reality (Figs. 7-10). Besides, it should be noted that the criterion used for extracting TMZs in different estuaries and seasons was exactly the same (TMZI > 0.2) and got a reasonable accuracy and better performance compared to the previous fixed TSS concentration or turbidity threshold (Fig. 11), which showed that TMZI has a higher adaptability and robustness.

The results indicated that there is great potential for optimizing the TMZI to distinguish and extract TMZs from multi-source satellite remote sensing, such as Sentinel, Aqua & Terra-MODIS and SeaWiFS, which also provides great help in establishing and developing a unified criterion for extracting TMZs effectively in different estuaries and different times throughout the world.

Code and data availability

All the Landsat remote sensing imageries are fully available at https://glovis.usgs.gov/ (USGS 1982; NASA 2001).

Author Contribution

The individual contributions and responsibilities of the authors are listed as follows: Chongyang Wang and Li Wang designed the research and wrote the paper; Chenghu Zhou and Dan Li guided the research process; Danni Wang, Qiong Zheng, Hao Jiang and Yangxiaoyue Liu collected and analyzed the data; Shuisen Chen, Ji Yang, Xia Zhou and Yong Li revised the manuscript, provided some comments and helped edit the manuscript. All authors have read and agreed to the published version of the manuscript.

Competing interests

The authors declare that they have no conflict of interest.

Acknowledgements

This work was funded jointly by National Natural Science Foundation of China (41801364), Natural Science Foundation of Guangdong Province (2021A1515012579), Key Special Project for Introduced Talents Team of Southern Marine Science and Engineering Guangdong Laboratory (Guangzhou) (GML2019ZD0301), Scientific Research Project approved by Department of Education of Guangdong Province (2019KQNCX209), Guangdong Innovative and Entrepreneurial Research Team Program (2016ZT06D336) and GDAS' Project of Science and Technology Development (2020GDASYL-20200104006, 2020GDASYL-20200302001, 2019GDASYL-0503001, 2019GDASYL-0301001 and 2019GDASYL-0501001). We would also like to thank USGS for providing the Landsat remote sensing imageries.

References

Asp, N.E., Gomes, V., Schettini, C.A.F., Filho, P.W.S., Siegle, E., Ogston, A.s., Nittrouer, C.A., Silva, J.N.S., Nascimento, W.R., Jr, Souza, S.R., Pereira, L.C.C., Queiroz, M.C., 2018. Sediment dynamics of a tropical tide-dominated estuary: Turbidity maximum, mangroves and the role of the Amazon River sediment load. Estuarine, Coastal and Shelf Science.

Attila, J., Kauppila, P., Kallio, K.Y., Alasalmi, H., Keto, V., Bruun, E., Koponen, S., 2018. Applicability of Earth Observation chlorophyll-a data in assessment of

https://doi.org/10.5194/gmd-2020-378
Preprint. Discussion started: 26 May 2021

water status via MERIS-With implications for the use of OLCI sensor. Remote Sensing of Environment. 212, 273-287.

Azhikodan, G., Yokoyama, K., 2019. Seasonal morphodynamic evolution in a meandering channel of a macrotidal estuary. Science of the Total Environment. 684, 281-295.

Brenon, I., Hir, P.L., 1999. Modelling the Turbidity Maximum in the Seine Estuary (France): Identification of Formation Processes. Estuarine, Coastal and Shelf Science. 49, 525-544.

Chen, S., Fang, L., Li, H., Chen, W., Huang, W., 2011. Evaluation of a three-band model for estimating chlorophyll-a concentration in tidal reaches of the Pearl River Estuary, China. ISPRS Journal of Photogrammetry and Remote Sensing. 68, 356-364.

Chen, S., Han, L., Chen, X., Li, D., Sun, L., Li, Y., 2015. Estimating wide range Total Suspended Solids concentrations from MODIS 250-m imageries: An improved method. ISPRS Journal of Photogrammetry and Remote Sensing. 99, 58-69.

Chen, X., Shen, Z., Yang, Y., 2016. Response of the turbidity maximum zone in the Yangtze River Estuary due to human activities during the dry season. Environmental Science and Pollution Research. 11, 1-16.

Feng, H., Cochran, J.K., Hirschberg, D.J., 2002. Transport and sources of metal contaminants over the course of tidal cycle in the turbidity maximum zone of the Hudson River estuary. Water Research. 36, 733-743.

https://doi.org/10.5194/gmd-2020-378
Preprint. Discussion started: 26 May 2021

Gebhardt, A.C., Schoster, F., Gaye-Haake, B., Beeskow, B., Rachold, V., Unger, D., Ittekkot, V., 2005. The turbidity maximum zone of the Yenisei River (Siberia) and its impact on organic and inorganic proxies. Estuarine, Coastal and Shelf Science. 65, 61-73.

Gong, S., Gao, A., Lin, J., Zhu, X., Zhang, Y., Hou, Y., 2017. Temporal-spatial distribution and its influencing factors of suspended particulate matters in Minjiang lower reaches and estuary. Journal of Earth Sciences and Evironment. 39(6), 826-836.

Grasso, F., Verney, R., Hir, P.L., Thouvenin, B., Schulz, E., Kervella, Y., Fard, I.K.P., Lemoine, J.-P., Dumas, F., Garnie, V., 2018. Suspended Sediment Dynamics in the Macrotidal Seine Estuary (France) - Part 1: Numerical Modeling of Turbidity Maximum Dynamics. Journal of Geophysical Research: Oceans. 123, 558-577.

Gregg, W.W., Casey, N.W., 2004. Global and regional evaluation of the SeaWiFS chlorophyll data set. Remote Sensing of Environment. 93, 463-479.

Huang, B., Hong, H., Ke, L., Cao, Z., 2005. Size-fractionated phytoplankton biomass and productivity in the Zhujiang River Estuary in China. Acta Oceanologica Sinica. 27, 180-186.

Jalón-Rojas, I., Schmidt, S., Sottolichio, A., Bertier, C., 2016. Tracking the turbidity maximum zone in the Loire Estuary (France) based on a long-term, high-resolution and high-frequency monitoring network. Continental Shelf Research. 117, 1-11.

https://doi.org/10.5194/gmd-2020-378
Preprint. Discussion started: 26 May 2021

Jiang, J., He, Q., Zhu, L., Lin, J., 2019. Analysis of hydrodynamic features of the North Passage in the turbidity maximum, Changjinag Estuary. Haiyang Xuebo. 41(1), 11-20.

Jiang, X., Lu, B., He, Y., 2013. Response of the turbidity maximum zone to fluctuations in sediment discharge from river to estuary in the Changjiang Estuary (China). Estuarine, Coastal and Shelf Science. 131, 24-30.

Kim, H.H., Ko, B.C., Nam, J.Y., 2016a. Predicting chlorophyll-a using Landsat 8 OLI sensor data and the non-linear RANSAC method –a case study of Nakdong River, South Korea. International Journal of Remote Sensing. 37, 3255-3271.

Kim, W., Moon, J.-E., Park, Y.-J., Ishizaka, J., 2016b. Evaluation of chlorophyll retrievals from Geostationary Ocean Color Imager (GOCI) for the North-East Asian region. Remote Sensing of Environment. 184, 482-495.

Kitheka, J.U., Mavuti, K.M., Nthenge, P., Obiero, M., 2016. The turbidity maximum zone in a shallow, well-flushed Sabaki estuary in Kenya. Journal of Sea Research. 110, 17-28.

Le, C., Hu, C., Cannizzaro, J., English, D., Muller-Karger, F., Lee, Z., 2013. Evaluation of chlorophyll-a remote sensing algorithms for an optically complex estuary. Remote Sensing of Environment. 129, 75-89.

Le, C., Li, Y., Zha, Y., Sun, D., Huang, C., Lu, H., 2009. A four-band semi-analytical model for estimating chlorophyll a in highly turbid lakes: The case of Taihu Lake, China. Remote Sensing of Environment. 113, 1175-1182.

https://doi.org/10.5194/gmd-2020-378
Preprint. Discussion started: 26 May 2021

Li, L., Ye, T., Wang, X., Xia, Y., 2019. Tracking the multidecadal variability of the surface turbidity maximum zone in Hangzhou Bay, China. International Journal of Remote Sensing. 1-22.

Liu, H., Huang, L., Tan, Y., Ke, Z., Liu, J., Zhao, C., Wang, J., 2017. Seasonal variations of chlorophyll a and primary production and their influencing factors in the Pearl River Estuary. Journal of Tropical Oceanography. 36, 81-91.

Liu, R., Wang, Y., Gao, J., Wu, Z., Guan, W., 2016. Turbidity maximum formation and its seasonal variations in the Zhujiang (Pearl River) Estuary, southern China. Acta Oceanologica Sinica. 35, 22-31.

Mitchell, S., 2013. Turbidity maxima in four macrotidal estuaries. Ocean & Coastal Management. 79, 62-69.

Mitchell, S., Akesson, L., Uncles, R., 2012. Observations of turbidity in the Thames Estuary, United Kingdom. Water and Environment Journal. 26, 511-520.

Montanher, O., Novo, E., Barbosa, C., Renno, C., Silva, T., 2014. Empirical models for estimating the suspended sediment concentration in Amazonian white water rivers using Landsat 5/TM. International Journal of Applied Earth Observation and Geoinformation, 29, 67-77.

Park, K., Wang, H.V., Kim, S.-C., Oh, J.-H., 2008. A Model Study of the Estuarine Turbidity Maximum along the Main Channel of the Upper Chesapeake Bay. Estuaries and Coasts. 31, 115-133.

https://doi.org/10.5194/gmd-2020-378
Preprint. Discussion started: 26 May 2021

Pozdnyakov, D., Shuchman, R., Korosov, A., Hatt, C., 2005. Operational algorithm for the retrieval of water quality in the Great Lakes. Remote Sensing of Environment. 97, 352-370.

Schubel, J., 1968. Turbidity maximum of the northern chesapeake bay. SCIENCE. 161, 1013-1015.

Shen, H., 1995. New understanding on the study of the maximum turbidity zone in estuaries of China. Advence in Earth Sciences. 10, 210-212.

Shen, H., He, S., Mao, Z., Li, J., 2001. On the turbidity maximum in the Chinese estuaries. Journal of Sediment Research. 1, 23-29.

Shi, W., Shen, H., Li, J., 1993. Review on the formation of estuarine turbidity maximum. Advence in Earth Sciences. 8, 8-13.

Shi, Z., Xu, J., Huang, X., Zhang, X., Jiang, Z., Ye, F., Liang, X., 2017. Relationship between nutrients and plankton biomass in the turbidity maximum zone of the Pearl River Estuary. Journal of Environmental Sciences. 57, 72-84.

Song, K., Li, L., Tedesco, L.P., Li, S., Duan, H., Liu, D., Hall, B.E., Du, J., Li, Z., Shi, K., Zhao, Y., 2013. Remote estimation of chlorophyll-a in turbid inland waters: Three-band model versus GA-PLS model. Remote Sensing of Environment. 136, 342-357.

Toublanc, F., Brenon, I., Coulombier, T., 2016. Formation and structure of the turbidity maximum in the macrotidal Charente estuary (France)_ Influence of fluvial and tidal forcing. Estuarine, Coastal and Shelf Science. 169, 1-14.

https://doi.org/10.5194/gmd-2020-378
Preprint. Discussion started: 26 May 2021

Uncles, R.J., Bloomer, N.J., Frickers, P.E., Griffiths, M.L., Harris, C., Howland, R.J.M., Morris, A.W., Plummer, D.H., Tappin, A.D., 2000. Seasonal variability of salinity, temperature, turbidity and suspended chlorophyll in the Tweed Estuary. The Science of the Total Environment. 251/252, 115-124.

Wai, O.W.H., Wang, C.H., Li, Y.S., Li, X.D., 2004. The formation mechanisms of turbidity maximum in the Pearl River estuary, China. Marine Pollution Bulletin. 48, 441-448.

Wan, Y., Wang, L., 2017. Numerical investigation of the factors influencing the vertical profiles of current, salinity, and SSC with in a turbidity maximum zone. International Journal of Sediment Research. 32, 20-33.

Wang, C., Chen, S., Li, D., Wang, D., liu, W., Yang, J., 2017a. A Landsat-based model for retrieving total suspended solids concentration of estuaries and coasts in China. Geoscientific Model Development. 10, 4347-4365.

Wang, C., Chen, S., Yang, J., Li, Y., Zhou, X., Li, D., Wang, D., 2020. Monitoring total suspended solids concentrations in estuaries based on remote sensing. Beijing: China Water & Power Press.

Wang, C., Li, D., Wang, D., Chen, S., 2017b. Detecting the Temporal and Spatial Changes of Suspended Sediment Concentration in Hanjiang River Estuary During the Past 30 Years Using Landsat Imageries. Research Journal of Environmental Science. 11, 143-155.

https://doi.org/10.5194/gmd-2020-378
Preprint. Discussion started: 26 May 2021

Wang, C., Li, W., Chen, S., Li, D., Wang, D., Liu, J., 2018. The spatial and temporal variation of total suspended solid concentration in Pearl River Estuary during 1987–2015 based on remote sensing. Science of the Total Environment. 618, 1125-1138.

Wang, C., Wang, D., Yang, J., Fu, S., Li, D., 2020b. Suspended Sediment within Estuaries and along Coasts: A Review of Spatial and Temporal Variations based on Remote Sensing. Journal of Coastal Research. doi:10.2112/JCOASTRES-D-19-00164.1.

Wang, C., Zhou, C., Chen, S., Xie, Y., Li, D., Yang, J., Zhou, X., Li, Y., Wang, D., Liu, Y., 2020a. Retrospect and perspective of the estuarine turbidity maximum zone researches. Chinese Science Bulletin. doi: 10.1360/TB-2020-0938.

Yan, D., Song, D., Bao, X., 2020. Spring-neap tidal variation and mechanism analysis of the maximum turbidity in the Pearl River Estuary during flood season. Journal of Tropical Oceanography. 39, 20-35.

Yang, J., Liu, W., 2015. Characteristics of the maximum turbidity zone in the lingdingyang-Pearl river estuary during the flood season in the recent 30 years. Pearl River Water Transport. 16, 58-62.

Yang, Y., Li, Y., Sun, Z., Fan, Y., 2014. Suspended sediment load in the turbidity maximum zone at the Yangtze River Estuary: The trends and causes. Journal of Geographical Sciences. 24, 129-142.

https://doi.org/10.5194/gmd-2020-378
Preprint. Discussion started: 26 May 2021

Geoscientific Model Development
Discussions

Yu, Q., Wang, Y., Gao, J., Gao, S., Flemming, B., 2014. Turbidity maximum formation in a well-mixed macrotidal estuary: The role of tidal pumping. Journal of Geophysical Research: Oceans. 119, 7705-7724.

Zhang, X., Chen, X., Dou, X., Zhao, X., Xia, W., Jiao, J., Xu, H., 2019. Study on formation mechanism of turbidity maximum zone and numerical simulations in the macro tidal estuaries. Advances in Water Science. 30, 84-92.